REPORT DOCUMENTATION PAGE

Form Approved OMB No. 0704-0188

1. REPORT DATE *(DD-MM-YYYY)*	2. REPORT TYPE	3. DATES COVERED *(From – To)*
01-05-2009	Final Report	1 November 2008 - 01-May-09

4. TITLE AND SUBTITLE

Chemical Reactivity as a Probe of Ionic-Liquid Surfaces

5a. CONTRACT NUMBER
FA8655-08-1-3079

5b. GRANT NUMBER

5c. PROGRAM ELEMENT NUMBER

6. AUTHOR(S)

Professor Kenneth McKendrick

5d. PROJECT NUMBER

5d. TASK NUMBER

5e. WORK UNIT NUMBER

7. PERFORMING ORGANIZATION NAME(S) AND ADDRESS(ES)
Heriot-Watt University
Riccarton Campus
Edinburgh EH14 4AS
United Kingdom

8. PERFORMING ORGANIZATION REPORT NUMBER
N/A

9. SPONSORING/MONITORING AGENCY NAME(S) AND ADDRESS(ES)

EOARD
Unit 4515 BOX 14
APO AE 09421

10. SPONSOR/MONITOR'S ACRONYM(S)

11. SPONSOR/MONITOR'S REPORT NUMBER(S)
Grant 08-3079

12. DISTRIBUTION/AVAILABILITY STATEMENT

Approved for public release; distribution is unlimited.

13. SUPPLEMENTARY NOTES

14. ABSTRACT

This report results from a contract tasking Heriot-Watt University as follows: The work will be similar to that which the group has pioneered in related studies of the reactions of O(3P) atoms with hydrocarbon liquids. It is based on laser-photolysis of a low pressure of a suitable O(3P) precursor (NO2 at 355 nm) above the surface of the liquid. This produces O(3P) atoms with a relatively broad, superthermal kinetic energy distribution, centred on 16 kJmol-1 with a FWHM of 26 kJmol-1.
The project will measure the relative reactivity of the series 1-alkyl-3-methylimidazolium ([Rmim], where R = Me, Et, Bu, Hex, Oct, Dec) [Im] salts by detecting relative OH yields by laser-induced fluorescence (LIF). The work will also compare the reactivity of one of the simpler members, [Emim], with the NO3- counter-ion, because this is the combination most commonly selected for theoretical studies. All reactivities will be calibrated against the 'benchmark' hydrocarbon liquid, squalane.
Guided by the results of the relative reactivity measurements, preliminary studies of the OH product internal and translational energy distributions for a selection of the ionic liquids will be carried out. The experiments are uniquely capable of providing this information, which helps to distinguish between the two limiting mechanisms seen in essentially all previous studies of reactive and inelastic scattering from hydrocarbons and some other liquids. One component is direct, dynamically controlled scattering at the outer layers of the liquid. The other is trapping-desorption, in which products are accommodated at the surface and take on near-thermal translational and rotational energy distributions. The balance between them is affected by the surface structure, in particular its penetrability and molecular roughness, whose dependence on the molecular structure of the [Rmim] will therefore be tested by measurement

15. SUBJECT TERMS
EOARD, ionic liquids, electrospray thrusters, laser induced flourescence

16. SECURITY CLASSIFICATION OF:			17. LIMITATION OF ABSTRACT	18, NUMBER OF PAGES	19a. NAME OF RESPONSIBLE PERSON
a. REPORT	b. ABSTRACT	c. THIS PAGE			BARRETT A. FLAKE
UNCLAS	UNCLAS	UNCLAS	UL	18	**19b. TELEPHONE NUMBER** *(Include area code)* +44 (0)1895 616144

Chemical Reactivity as a Probe of Ionic-Liquid Surfaces

Project funded under EOARD contract No. FA8655-08-1-3079

Final Report, 30 April 2009

*Carla Waring, Paul A J Bagot, Matthew L Costen and Kenneth G McKendrick**

School of Engineering and Physical Sciences, Heriot-Watt University, Edinburgh EH14 4AS, UK

k.g.mckendrick@hw.ac.uk

TABLE OF CONTENTS

LIST OF FIGURES

SUMMARY

We have successfully investigated the gas-liquid interfacial reactivity of superthermal O(^{3}P) atoms with a range of ionic liquids. Direct reaction at the outer layer of the liquid has been identified as the dominant mechanism. We have also observed an interesting non-linear dependence of the reactivity on the chain-length. This clearly indicates the influence of chainlength-dependent surface structure on the availability of abstractable H atoms, which would be worthy of further research.

INTRODUCTION

Ionic Liquids (ILs) are a class of salts which have melting points below ~100°C. They are comprised solely of ions, and have a number of unique physical and chemical properties such as negligible vapour pressure, low volatility and high thermal stability. These features make ILs attractive as green solvents, replacing traditional organic chemicals[1], and potentially useful in a varied range of applications spanning catalysis[2], fuel cells[3], nanoparticle formation[4,5], anti-electrostatic coatings[6], vapor detection[7] and of particular relevance to the current study, electrospray thrusters[8,9].

While there are at least 10^6 potential primary ILs readily available for research[10], one of the most-studied classes of ILs is based on 1,3-dialkyl imidiazolium cations. Adjusting the length of the alkyl groups on these offers a convenient method of tuning the properties of the liquid. Alkyl groups up to 12 carbon atoms in length are routinely investigated[11].

Many of the applications for ionic liquids are dependent on the detailed structure of the gas-liquid interface. The large organic cations and sometimes anions are responsible for their desired low melting points; however they also make a complete understanding of the interfacial structure much more difficult than simple salts such as NaCl, as it is no longer clear whether the gas-liquid interfacial structure is equivalent to that in the bulk. Experimentally, this aspect of ILs has been investigated by a number of groups, utilizing techniques including direct recoil spectroscopy (DRS)[11], sum-frequency generation vibrational spectroscopy[12,13,14], x-ray photoelectron spectroscopy[15,16] and neutron reflectivity[17]. Alongside this experimental effort, molecular dynamics simulations of 1,3-dialkyl imidiazolium cations with several types of anion have investigated a range of IL properties of both bulk and interfacial regions[18,19,20,21,22,23,24,25].

A common observation in the current literature is that the interfacial structure differs from the bulk, with the longest alkyl chain on the cation noted to project out into the vacuum[12,13,26], even forming

multilayer lamellar-like structures with both charges localized between alkyl-rich layers[17]. However there is far from a universal consensus on this, with some studies suggesting that no ion segregation takes place, with the alkyl groups pointing along or even down into the liquid[11]. Recent work has suggested that the presence of water can play a role in determining surface properties[14,27], while it has been suggested that neglecting polarizability effects has hampered MD simulations[23].

In the current study, the aspect we address is the interfacial reactivity of [RMIM] [Im] (representing 1-alkyl-3-methylimidazolium bis(trifluoromethylsulfonyl)imide) ionic liquids with ground-state atomic oxygen, O(^{3}P). One of the lower members of this series, [EMIM] (1-ethyl-3-methylimidazolium) [Im], has specifically been earmarked as a candidate for thruster systems[8]. This reaction is of particular relevance to space applications because O(^{3}P) is the majority atmospheric species at the altitudes (200-700 km) of low-Earth orbit (LEO). Constituents of thrusters will therefore be subject to reaction with O(^{3}P) at hyperthermal collision energies because of the orbital motion of the spacecraft through the stationary atmosphere[28]. In our experiments, we use a laser-photolysis based method to study this reaction, monitoring the relative OH product yields from a range of [RMIM] [Im] salts. This method has been pioneered successfully in related studies of the reactions of O(^{3}P) atoms with hydrocarbon liquids[29,30,31,32,33,34] , and has proven to be a sensitive probe of the liquid surface structure.

We aim here to measure the relative reactivity of [RMIM] [Im] for a series of [RMIM] cations, where the R chainlength was anticipated to span a range from C_1 to C_{10}. All reactivities will be calibrated against the 'benchmark' hydrocarbon liquid, squalane. Aside from the relative reactivity measurements, we shall also carry out preliminary studies of the OH product internal and translational energy distributions for a selection of the ionic liquids. This information helps to distinguish between the two limiting mechanisms seen in essentially all previous studies of reactive and inelastic scattering from hydrocarbons and some other liquids. One component is direct, dynamically controlled impulsive scattering (IS) at the outer layers of the liquid. The other is trapping-desorption (TD), in which products are accommodated at the surface and take on near-thermal translational and rotational energy distributions. The balance between them is affected by the surface structure, whose dependence on the molecular structure of the [RMIM] will therefore be tested by our measurements.

METHODS

The experimental set-up has been adapted from that described previously for the investigation of the reaction dynamics of $O(^3P)$ and liquid hydrocarbons.[29,30,31,32,33,34] Central to the apparatus is a 5 cm-diameter stainless steel wheel (Fig. 1), housed within a vacuum chamber. The wheel is partially immersed in a copper bath filled with the liquid under investigation, rotating at 0.5 Hz generating a continually refreshed liquid surface. The [RMIM] [Im] ionic liquids used were custom-synthesized by Dr John Slattery, University of York. In practice, four ionic liquids have been investigated so far [EMIM] [Im], [BMIM] [Im], [PMIM] [Im] and [DMIM] [Im] (see Fig. 2 for definitions), with structures differing only in the length of the 1-alkyl chain. The liquid hydrocarbon squalane ($C_{30}H_{62}$, 2,6,10,15,19,23-hexamethyltetracosane) for which the interfacial reactivity with $O(^3P)$ has been extensively studied by us previously[29,30,31,33] was used as a standard to quantify the relative reactivity of the ionic liquids. The inert perfluoropolyether (PFPE) Krytox® 1506 (F-$[CF(CF_3)CF_2O]_{14ave}$-CF_2CF_3,) was also used to check for artefacts due to OH that might be generated in processes other than reaction at the liquid surface.

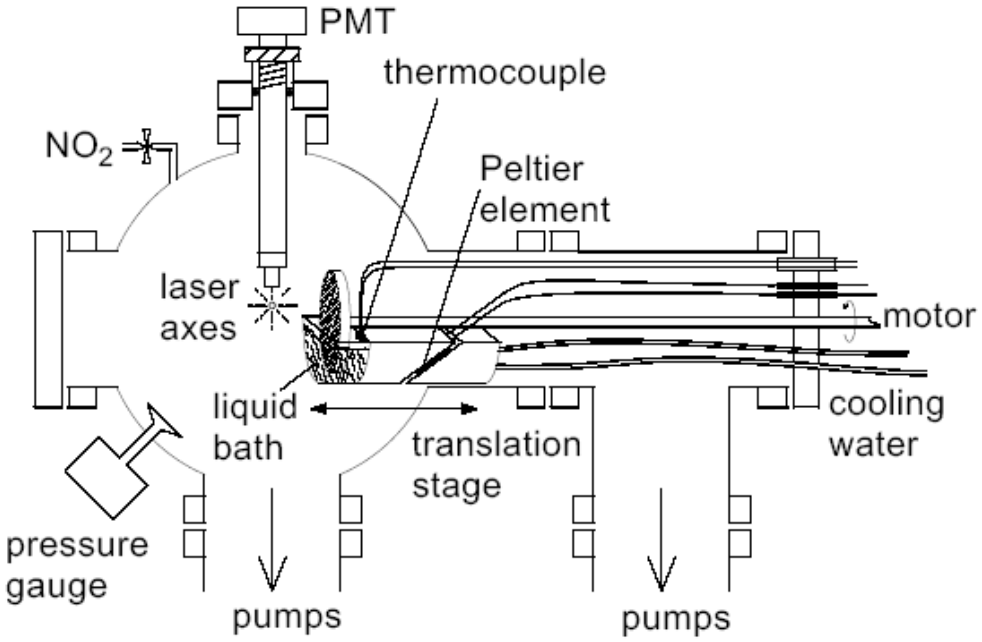

Fig. 1 Side elevation of experimental chamber

Prior to each experiment, the ionic liquid sample was heated using a Peltier heating element to (70±3) ºC for ~24 hours under vacuum, to ensure thorough de-gassing and to remove any residual water prior

to use. The chamber was evacuated using a cryo-cooled diffusion pump and a turbo-pump both backed by rotary pumps fitted with a cryo and a foreline trap filled with activated alumina to prevent any hydrocarbon-containing species from contaminating the ionic liquids.

The O(^{3}P) atoms were generated by photolyzing a carefully controlled pressure (nominally 1 mTorr) of NO_2 (BOC, 98.3%) at a fixed distance of 4 mm above the liquid surface. This was achieved using the third harmonic of a Nd:YAG laser (Continuum Surelite II-10), supplying 355 nm light pulses of width 4-6 ns at 10 Hz. The laser energy was maintained at a constant value of around 100 mJ per pulse, measured upon entry to the vacuum chamber. The photolysis beam (4 mm diameter) counter-propagated the probe beam, passing at the same carefully controlled distance from the surface. The spatial distribution of the O(^{3}P) produced in this manner is described by an anisotropy parameter, $\beta = +0.7$ [35]. The photolysis laser was horizontally polarized, so roughly half of the O(^{3}P) was directed toward the liquid surface. The collision energy of the O(^{3}P) atoms is broadly distributed around an average value of 15.8 kJ mol^{-1} (with a FWHM of 26 kJ mol^{-1}) in the laboratory frame, corresponding to an average speed of 1340 ms^{-1} [35].

When the O(^{3}P) atoms impact on the liquid surface, some of them extract hydrogen atoms, generating OH $X^2\Pi$ radicals. A fraction of these escape from the surface and are detected by laser-induced fluorescence (LIF). In the current work we have only attempted to detect vibrational ground-state OH on their respective $A^2\Sigma^+$-$X^2\Pi$ (1,0) bands using a Nd:YAG (Continuum Surelite II-10) pumped dye laser (Sirah Cobra Stretch). This supplied ca. 1 mJ, 4-6 ns pulses, again measured at the entrance to the vacuum chamber. The returning *A*-*X* fluorescence was collected by a liquid light guide (Ultrafine Technology, Ltd.) mounted 2 cm directly above the common laser axis. The fluorescence passed through custom interference filters before being converted into a signal by a photomultiplier tube (PMT, Electron Tubes Ltd.). This signal was in turn digitized and passed to a PC, which collected data and controlled the wavelength and timing of the lasers using custom-written LabVIEW® programs.

As explained fully below, experiments could be split into two basic types. The first were *appearance profiles*, acquired by varying the time delay between the photolysis and probe lasers to gain information on the translational energy of the escaping OH species in a particular rotational (and fine-structure and Λ-doublet) state of *v'* = 0. The second were LIF *excitation spectra*, acquired by scanning the wavelength of the probe laser at a fixed photolysis-probe delay. In all cases in the current work this was at the peak of the appearance profiles (typically 8 μs). These spectra yield information on the product rotational state distributions. To extract nascent populations, the spectra were compared with those from a known 'thermalized' distribution, as we have described in our previous work.[29,30,31,33] These 'thermal'

excitation spectrum were recorded at a typical pressure of 0.5 Torr of N_2 (~1 mTorr NO_2) and a photolysis-probe delay of 30 μs, corresponding to approximately 150 collisions based on a typical gas-kinetic collision rate constant of 10^7 $Torr^{-1}$ s^{-1}.

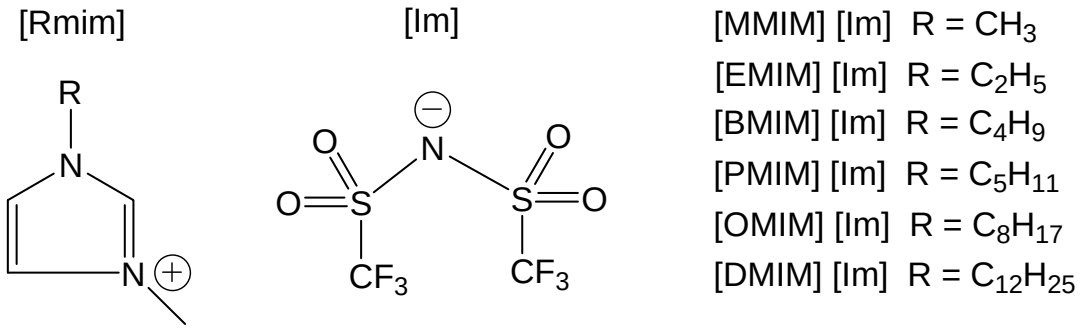

Fig. 2 Chemical structures and nomenclature used for the 1-alkyl-3-methylimidazolium based ionic liquids.

RESULTS

Relative reactivity measurements

To quantify the relative reactivity of the series of [RMIM] [Im] liquids we measured each of their reactivities against the well-studied reference liquid, squalane. Appearance profiles were recorded by fixing the probe laser wavelength on a specific OH *A-X* transition, usually the $Q_1(1)$ transition, and varying the delay time between the photolysis and probe laser. There was a small constant background signal, likely caused by probe-induced photolysis of a minor OH-containing impurity in the NO_2, which underlies each appearance profile. Therefore, a background profile was recorded for each appearance profile by blocking the photolysis laser while keeping all other factors equal. This background signal was then subtracted from its corresponding profile to give true OH appearance profiles from the reaction of $O(^3P)$ atoms only.

For a given ionic liquid, appearance profiles (typically 10 profiles) were recorded from the thoroughly degassed liquid at 25ºC. We took particular care that factors such as probe laser energy, NO_2 precursor pressure and wheel-laser axes distance remained constant. The wheel would then be removed immediately and cleaned thoroughly and the bath re-filled with the squalane reference. Appearance profiles would then be recorded from squalane under otherwise essentially identical conditions. Preliminary heating and degassing has not been found to be necessary for squalane, as expected, since it is unlikely to contain any significant amounts of dissolved water. The relative reactivity of each liquid

compared with the squalane reference is then taken to be the ratio of the peaks in the respective appearance profiles.

An important test of the experimental procedure was to confirm that no OH was detected from an inert liquid containing no abstractable hydrogens. We used PFPE for this purpose. As in the case of the ionic liquids, the PFPE was heated to 70ºC for ~24 hrs before the experiments and appearance profiles were recorded, as described above, from PFPE and the squalane reference. These appearance profiles are shown in Fig. 3(e). The profiles for squalane are as expected from our previous work. They contain a characteristic initial 'dead time' as the $O(^3P)$ atoms travel to the liquid surface and the OH returns to the probe volume. The OH signal rises sharply, reaching a peak at a time delay consistent with the known distances, the average incoming $O(^3P)$ speed of 1340 ms^{-1}, and sensible recoil speeds for directly scattered OH (see below). The appearance profiles from PFPE however are in stark contrast, with no perceptible OH present. This confirms that there is indeed no significant production of spurious OH.

This experimental procedure was repeated for [EMIM] [Im] (Fig. 3(a)). There was again effectively no OH detected within the sensitivity of the measurement. The small apparently negative signal in Figs. 3(a) and (e) at early time delays is an artefact from the imperfect subtraction of a background due to the photolysis laser which underlies all profiles. We have estimated an upper limit to the relative reactivity of [EMIM] [Im] compared with squalane as 1:0.0014 (see Table 1).

Since we were unable to detect OH reaction products from the [EMIM] [Im] liquid, we did not expect reaction with [MMIM] [Im] (M = methyl) to yield detectable amounts of OH either. For this reason, [MMIM] [Im] was not pursued in the current study.

Therefore, in the light of these results, to give the best chance of identifying an [RMIM] [Im] with finite reactivity, we examined longer alkyl chains. The longest practical chainlength that retains the physical properties required for the experiment and is synthetically convenient to prepare is [DMIM] (D = dodecyl). In contrast to [EMIM] [Im], a significant OH signal was detected from [DIMI] [Im], as shown in Fig. 3(d). The relative reactivity of squalane to [DMIM] [Im] is quantified as 1:0.62±0.06 (Table 1.). Having successfully measured the relative reactivity of the ionic liquids at the practical extremes of alkyl chain lengths, we proceeded to examine intermediate chainlengths. To date the reactivity of [BMIM] [Im] (B = butyl) and [PMIM] [Im] (P = pentyl) have also been measured and the relevant reactivity ratios are given in Table 1.

Fig. 4 summarises the relative reactivity of all the ionic liquids studied as a function of the number of CH_2 units in the 1-alkyl chain. (This measure is selected because we expect the more reactive,

secondary CH_2 units to generate the majority of the signal, as discussed below.) As might be expected, the reactivity varies with alkyl chain length, but very interestingly this increase is clearly non-linear with the number of CH_2 units. It is our intention to measure additional intermediate points to further characterize this variation. A sample of [OMIM] [Im] (O = octyl) has been synthesized, but requires further work to achieve the desired purity. We intend to complete the measurements on [OMIM] [Im] beyond the grant period.

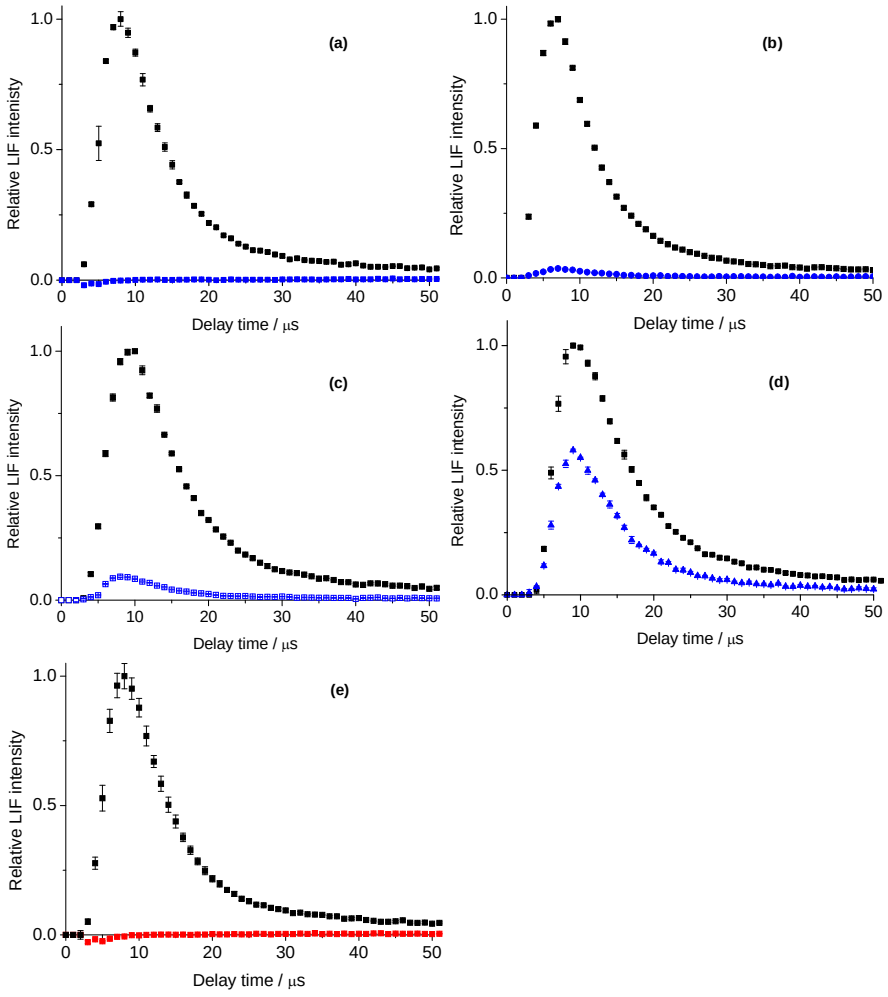

Fig. 3 Representative OH appearance profiles recorded on the $Q_1(1)$ line of the OH A-X (1,0) band. Background signals have been subtracted as described in the text. Squalane (black squares) was used as a reference in all cases. The liquids examined were **(a)** [EMIM] [Im] (blue squares), **(b)** [BMIM] [Im] (blue circles), **(c)** [PMIM] [Im] (blue open squares), **(d)** [DMIM] [Im] (blue triangles), **(e)** PFPE (red squares). Bath temperature = 298 K; $p(NO_2)$ ~ 1 mTorr; surface-probe laser distance = 4 mm.

Cation	Squalane: ionic liquid			
	Measurement 1	**Measurement 2**	**Measurement 3**	**Mean**
[EMIM]	1:0.00125	1:0.00153	-	1:0.0014†
[BMIM]	1:0.037	1:0.036	1:0.041	1:0.038±0.004
[PMIM]	1:0.061	1:0.094	1:0.100	1:0.085±0.024
[DMIM]	1:0.58	1:0.60	1:0.67	1:0.62±0.06

Table. 1 Summary of repeated independent measurements of relative reactivity ratios of a series of [RMIM] [Im] ionic liquids with O(^{3}P), each compared to a squalane standard. Error quoted is the 2σ standard error in the mean. †Estimated upper limit on reactivity.

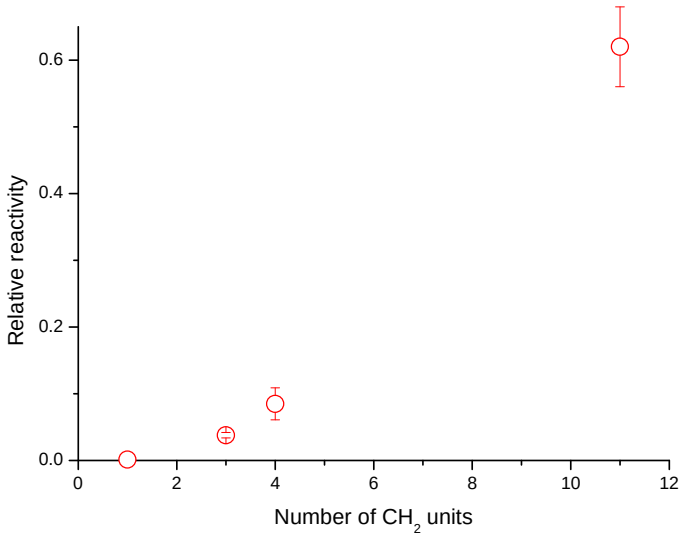

Fig. 4 Relative reactivity towards O(^{3}P) (compared to squalane reference) as a function of number of CH_2 units in the 1-alkyl chain of a series of [RMIM] [Im] ionic liquids. Error bars show the combined errors from the 2σ standard error in the mean of the relative reactivity measurements for each liquid.

O(^{3}P) + [DMIM] [Im] reaction mechanism

The high reactivity and corresponding high signal-to-noise achieved for [DMIM] [Im] allowed us to investigate this system in more detail. The [DMIM] [Im] appearance profile from Fig. 3(d) has been re-presented in Fig. 5, with its peak normalized to that of the squalane profile. The overall shape of both profiles is relatively similar, but there are subtle differences. In particular, the [DMIM] [Im] profile decays faster than that from squalane, implying a correspondingly smaller proportion of slower OH.

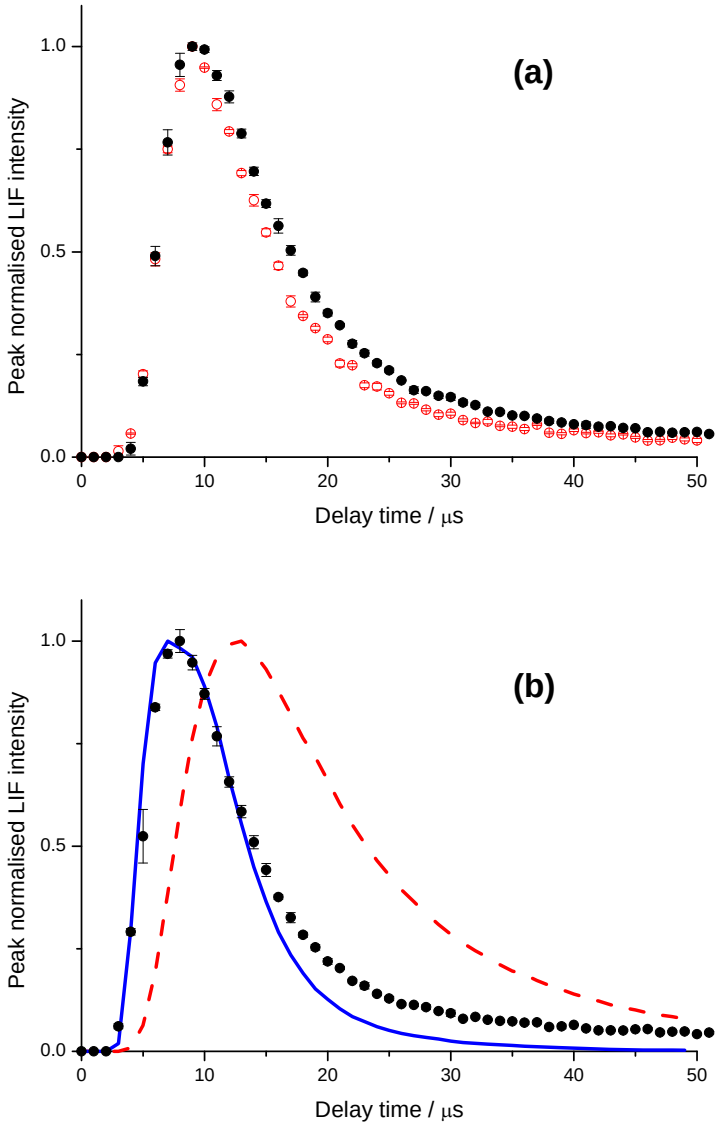

Fig. 5 (a) Representative appearance profiles of OH (v' = 0) peak-normalised LIF signals for squalane (black filled circles) and [DMIM] [IM] (red open circles). Profiles recorded on $Q_1(1)$ line of the OH A-X (1,0) band, shown following background subtraction as described in the text. Bath temperature = 298 K; $p(NO_2)$ ~ 1 mTorr; surface-probe laser distance = 4 mm. **(b)** Representative appearance profiles of OH (v' = 0) peak normalised LIF signals for squalane (black filled circles), Monte Carlo simulations of a direct (blue solid line) and thermal (red dashed line) component, as described in the text.

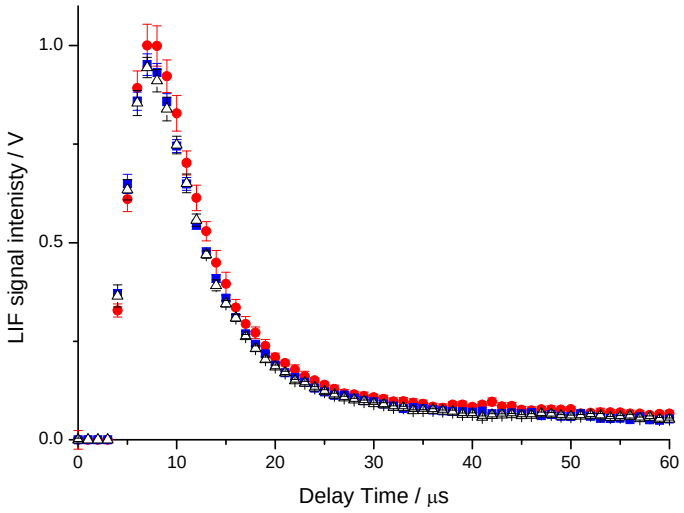

Fig. 6 Measured appearance profiles of OH (v' = 0) raw LIF signals for [DMIM] [Im] recorded at 298 K (blue squares), 323 K (black triangles) and 343 K (red circles). Profiles recorded on $Q_1(1)$ line of the OH A-X (1,0) band, shown following background subtraction as described in the text. $p(NO_2)$ ~ 1 mTorr; surface-probe laser distance = 4 mm.

Appearance profiles from [DMIM] [Im] were also recorded at three different liquid temperatures (Fig. 6), 298 K, 323 K and 343 K. Great care was taken to ensure consistency in other experimental parameters such as precursor pressure and probe laser energy, etc. It is clear that neither the peak height nor shape of the profile is significantly affected by varying the liquid temperature, with any differences in either absolute reactivity or the shapes of the profiles lying within the statistical uncertainties (as represented by the error bars).

We have also recorded nascent LIF excitation spectra from the [DMIM] [Im] ionic liquid, at the single photolysis-probe delay of 8 μs, close to the peak of the profiles in Fig. 3(d). A representative spectrum is shown in Fig. 7. As in our previous work, the spectra were analyzed by constructing Boltzmann plots from which effective temperatures could be extracted. Rotational temperatures were assigned to the six main branches P_1, Q_1, R_1 and P_2, Q_2, R_2. These temperatures were than averaged, giving an overall rotational temperature (Table 2) for each of the F_1 and F_2 spin-orbit manifolds. These were then averaged together with a weighting according to their relative populations in a 300 K thermal sample i.e. 70% F_1 and 30% F_2. The relative intensities of lines in the nascent spectrum (Fig. 7(a)) can be seen to be close to those in the thermal calibration spectrum (Fig. 7(b)). This naturally resulted in a fitted temperature close to thermal, at 309±8 K.

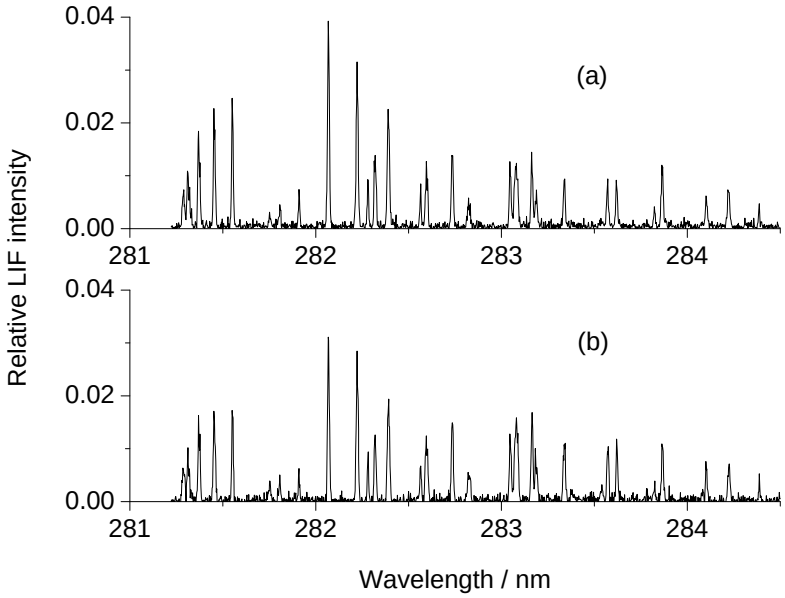

Fig. 7 Representative OH *A*-*X* (1,0) excitation spectra from [DMIM] [Im]. **(a)** Thermal spectrum recorded at a photolysis-probe laser delay of 30 μs, p(NO_2) ~ 1 mTorr and $p(N_2)$ ~ 0.5 Torr. **(b)** Nascent spectrum recorded at a photolysis-probe laser delay of 8 μs, probe laser-liquid surface distance = 4 mm $p(NO_2)$ ~ 1 mTorr.

	Run 1	**Run 2**	**Run 3**	**Run 4**	**Average**
F_1 Manifold	300 K	286 K	327 K	286 K	(300±10)K
F_2 Manifold	346 K	326 K	341 K	304 K	(329±9)K
Overall average					**(309±8)K**

Table. 2 Rotational temperatures of nascent OH (v' = 0) formed by reaction of (O^3P) atoms with [DMIM] [Im], measured at a photolysis-probe delay of 8 μs. Error quoted is the 1σ standard error in the mean.

DISCUSSION

A primary discovery from this work is that $O(^3P)$ atoms, with an average collision energy of 15.8 kJ mol^{-1}, react with [RMIM] [Im] ionic liquid surfaces and produce measurable quantities of free OH in the gas phase. In this respect we have shown that our method is indeed capable of acting as a "chemical probe" of the interfacial structure.

Aside from this basic result, the experimental data are sufficient to gain an understanding of both the mechanism of the reaction, and aspects of the liquid surface structure for the range of ILs explored.

Considering the mechanism first, we note from the appearance profiles that the majority of the OH detected from [DMIM] [Im] is travelling faster than it would be if formed via a trapping desorption mechanism. We have demonstrated this quantitatively in Fig. 5(b). This contains Monte Carlo simulations generated using a procedure we have described in detail previously.[36] Both thermal, trapping desorption (TD) and direct, impulsively scattered (IS) components have been simulated. The TD component is clearly too slow to explain the majority of the observed OH from either squalane or [DMIM] [Im]. In particular, it fails completely to account for the fastest OH at the sharp rising edge. In contrast, the IS component matches this component of both observed profiles very well. We have estimated previously[36] that the IS component accounts for at least 70% of the overall yield from squalane. It can be inferred from Fig. 5(a) that this component is somewhat higher from [DMIM] [Im], which has a trailing edge that drops more rapidly than for squalane, consistent with a smaller contribution from the slower TD component.

Further confirmation that the dominant mechanism with [DMIM] [Im] is direct scattering, with only one or at most a few collisions between the O/OH species and the liquid molecules, comes from the lack of any dependence on liquid temperature of the OH yield and the shape of the appearance profile, as shown in Fig. 6. If the $O(^3P)$ atoms had been initially trapped and gone on to react with the surface in a thermally activated mechanism, given the known activation energies for H abstraction from alkyl groups,[37, 38] the reactivity would have increased very markedly with liquid temperature. Similarly, if the desorbing OH contained a large component of thermally desorbing molecules, the appearance profile would reflect the change in the Maxwell Boltzmann distribution of translational energies as a function of temperature. Perhaps the only direct evidence for a contribution from a trapping desorption mechanism to the observed OH from [DMIM] [Im] might be the near thermal rotational distributions in Table 2. These are measured at the peak of the profiles where the TD component is predicted to be making a partial contribution (Fig. 5b). However, the relatively modest rotational energy release in this

class of reactions[37] makes the temperatures fairly insensitive to the proportion of the different reaction mechanisms.

A key goal in this study was to assess the effect of hydrocarbon chain length in [RMIM] [Im] on the relative reactivity. In Fig. 4, we find that increasing the chain length along the series [EMIM]→[DMIM] results in a non-linear increase in the reactivity of the ionic liquid to O(^{3}P) atoms. The impulsive nature of the majority reaction mechanism means that the observed OH yield must reflect rather directly the proportion of alkyl groups in the outermost layers of the liquid surface.

In interpreting these yields, we note that the activation energies for the corresponding abstraction reactions of O(^{3}P) with hydrocarbons in the gas phase are known to be strongly correlated with the strength of the C-H bond.[37, 38] We therefore expect that the secondary CH_2 units will dominate the reactivity of the R chains of the [RMIM] [Im] ionic liquids at the collision energies of our experiments. Similarly, secondary and tertiary units will make the major contribution for the squalane reference. Some support for this assumption comes from the very low reactivity of [EMIM] [Im], suggesting that the methyl group on the 3-position and the terminal methyl of the R = ethyl group contribute little to the reactivity. From previous work[39], we have estimated that the probability of an incoming O(^{3}P) atom colliding with a secondary or tertiary hydrogen atom on squalane (averaged over all incoming angles) is around 0.55. Therefore, comparing squalane with the most reactive ionic liquid, [DMIM] [Im] (as shown in Fig. 3), suggests that approximately 33% of the [DMIM] [Im] surface is composed of abstractable secondary hydrogens. This would provide an interesting absolute test of MD simulations of the [DMIM] [Im] surface structure. In more qualitative terms, our results agree with the interpretation of those other experiments[12,13,17] and simulations[26] that indicate that alkyl groups project outwards into the outer layers of the interface. However, the greater than linear increase in reactivity we have observed is not necessarily consistent in detail with previous angle-resolved XPS measurements of the surface composition of these [RMIM][Im] ILs[16]. This XPS study indicated surface enrichment of the aliphatic side-chains when 4 or more carbon atoms were present. Further work with additional chains of different lengths would be needed to test this proposition in detail using our methods. The yield of OH will also be dependent on the orientation of the alkyl chains, so quantitative comparisons with the results of other methods or predictions will require careful modeling. Nevertheless, our results serve to highlight once again the subtle complexity of the interfacial structures of such liquids.

FUTURE PROSPECTS

In future work, we plan to complete the investigation of the effect of different chain lengths on the reactivity of [RMIM] [Im] liquids with $O(^3P)$. We intend to present our findings at the 30th International Symposium on Free Radicals meeting in Finland in July 2009, and submit a paper to the special issue of the Journal of Physical Chemistry associated with this meeting.

ACKNOWLEDGEMENTS

We thank Dr. J. Slattery of University of York for his contribution in synthesizing the ionic liquids for these experiments.

REFERENCES

1 J. D. Holbrey and K. R. Seddon, *Clean Products and Processes*, 1999, **1**, 223.

2 R. Sheldon, *Chem. Commun.*, 2001, 2399.

3 E. Cho, J. S. Park, S. S. Sekhon, G. G. Park, T. H. Yang, W. Y. Lee, C. S. Kim, and S. B. Park, *J. Electrochem. Soc*., 2009, **156**, B197.

4 J. Dupont, G. S. Fonseca, A. P. Umpierre, P. F. P. Fichtner, and S. R. Teixeira, *JACS*, 2002, **124**, 4228.

5 C. W. Scheeren, G. Machado, S. R. Teixeira, J. Morais, J. B. Domingos, and J. Dupont, *J. Phys. Chem. B*, 2006, **110**, 13011.

6 J. Pernak, A. Czepukowicz, and R. Poźniak, *Ind. Eng. Chem. Res.*, 2001, **40**, 2379.

7 C. Liang, C.-Y. Yuan, R. J. Warmack, C. E. Barnes, and S. Dai, *Anal. Chem.*, 2002, **74**, 2172.

8 Y.-H. Chiu, G. Gaeta, D. J. Levandier, R. A. Dressler, and J. A. Boatz, *Int. J. Mass Spectrom.*, 2007, **265**, 146.

9 I. Romero-Sanz, R. Bocanegra, J. Fernandez de la Mora, and M. Gamero-Castaño, *J. Appl. Phys.*, 2003, **94**, 3599.

10 N. V. Plechkova and K. R. Seddon, *Chem. Soc. Rev.*, 2008, **37**, 123.

11 G. Law, P. R. Watson, A. J. Carmichael, and K. R. Seddon, *Phys. Chem. Chem. Phys.*, 2001, **3**, 2879.

12 C. S. Santos and S. Baldelli, *J. Phys. Chem. B*, 2007, **111**, 4715.

13 T. Iimori, T. Iwahashi, H. Ishii, K. Seki, Y. Ouchi, R. Ozawa, H. Hamaguchi, and D. Kim, *Chem. Phys. Lett.*, 2004, **389**, 321.

14 J. Sung, Y. Jeon, D. Kim, T. Iwahashi, T. Iimori, K. Seki, and Y. Ouchi, *Chem. Phys. Lett.*, 2005, **406**, 495.

15 E. F. Smith, I. J. Villar Garcia, D. Briggs, and P. Licence, *Chem. Commun.*, 2005, 5633.

[16] K. R. J. Lovelock, C. Kolbeck, T. Cremer, N. Paape, P. S. Schulz, P. Wasserscheid, F. Maier, and H.-P. Steinrück, *J. Phys. Chem. B*, 2009, **113**, 2854.
[17] J. Bowers and M. C. Vergara-Gutierrez, *Langmuir*, 2004, **20**, 309.
[18] T. I. Morrow and E. J. Maginn, *J. Phys. Chem. B*, 2002, **106**, 12807.
[19] Y. Wang and G. A. Voth, *J. Phys. Chem. B*, 2006, **110**, 18601.
[20] T. Yan, C. J. Burnham, M. G. Del Pópolo, and G. A. Voth, *J. Phys. Chem. B*, 2004, **108**, 11877.
[21] J. Picálek and J. Kolafa, *J. Mol. Liq.*, 2007, **134**, 29.
[22] M. H. Ghatee and Y. Ansari, *J. Chem. Phys.*, 2007, **126**, 154502.
[23] E. Sloutskin, R. M. Lynden-Bell, S. Balasubramanian, and M. Deutsch, *J. Chem. Phys.*, 2006, **125**, 174715.
[24] S. M. Urahata and M. C. Ribeiro, *J. Chem. Phys.*, 2004, **120**, 1855.
[25] R. M. Lynden-Bell, *Molec. Phys.*, 2003, **101**, 2625.
[26] B. L. Bhargava and S. Balasubramanian, *JACS*, 2006, **128**, 10073.
[27] J. M. Gottfried, F. Maier, J. Rossa, D. Gerhard, P. S. Schulz, P. Wasserscheid, and H. P. Steinruck, *Z. Phys. Chem.*, 2006, **220**, 1439.
[28] L. J. Leger and J. T. Visentine, *J. Spacecr. Rockets*, 1986, **23**, 505.
[29] H. Kelso, S. P. K. Köhler, D. A. Henderson, and K. G. McKendrick, *J. Chem. Phys.*, 2003, **119**, 9985.
[30] S. P. K. Köhler, M. Allan, H. Kelso, D. A. Henderson, and K. G. McKendrick, *J. Chem. Phys.*, 2005, **122**, 024712.
[31] S. P. K. Köhler, M. Allan, M. L. Costen, and K. G. McKendrick, *J. Phys. Chem. B*, 2006, **110**, 2771.
[32] M. Allan, P. A. J. Bagot, S. P. K. Köhler, M. L. Costen, and K. G. McKendrick, *Phys. Scr.*, 2007, **76**, C42.
[33] M. Allan, P. A. J. Bagot, M. L. Costen, and K. G. McKendrick, *J. Phys. Chem. C*, 2007, **111**, 14833.
[34] M. Allan, P. A. J. Bagot, R. E. Westacott, M. L. Costen, and K. G. McKendrick, *J. Phys. Chem. C*, 2008, **112**, 1524.
[35] R. P. Baker, M. L. Costen, G. Hancock, G. A. D. Ritchie, and D. Summerdeld, *Phys. Chem. Chem. Phys.*, 2000, **2**, 661.
[36] C. Waring, P. A. J. Bagot, M. T. Räisänen, M. L. Costen, and K. G. McKendrick, *J. Phys. Chem. A*, 2009, **113**, 4320.
[37] F. Ausfelder and K. G. McKendrick, *Progress in Reaction Kinetics and Mechanism*, 2000, **25**, 299.
[38] D. Troya, *J. Phys. Chem. A*, 2007, **111**, 10745.
[39] S. P. K. Köhler, S. K. Reed, R. E. Westacott, and K. G. McKendrick, *J. Phys. Chem. C*, 2006, **110**, 11717.